

First-order phase transitions in ferromagnet/superconductor layered structures

Paul H. Barsic,^{1,*} Oriol T. Valls,^{2,†} and Klaus Halterman^{3,‡}

¹*School of Physics and Astronomy and Minnesota Supercomputer Institute, University of Minnesota, Minneapolis, Minnesota 55455, USA*

²*School of Physics and Astronomy, University of Minnesota, Minneapolis, Minnesota 55455, USA*

³*Physics and Computational Sciences, Research and Engineering Sciences Department, Naval Air Warfare Center, China Lake, California 93555, USA*

(Received 6 December 2005; revised manuscript received 3 February 2006; published 24 April 2006)

We study the thermodynamics of clean structures composed of superconductor (S) and ferromagnet (F) layers and consisting of one or more SFS junctions. We use fully self-consistent numerical methods to compute the condensation free energies of the possible order parameter configurations as a function of temperature T . As T varies, we find that there are phase transitions between states characterized by different junction configurations (denoted as “0” or “ π ” according to the phase difference of the order parameter in consecutive S layers). We show that these transitions are of first order. We calculate the associated latent heats and find them to be measurable.

DOI: [10.1103/PhysRevB.73.144514](https://doi.org/10.1103/PhysRevB.73.144514)

PACS number(s): 74.45.+c, 74.25.Bt, 74.78.Fk

I. INTRODUCTION

A plethora of new ideas and devices has been emerging from the study of nanostructures as they pertain to the field of spintronics.¹ An important part of this development has occurred through the study of the rich and varied phenomena that occur² in heterostructures involving superconductors (S) and ferromagnets (F).

The physics of such F/S heterostructures is dominated by the proximity effects that arise from the competition between superconducting and magnetic orderings in the materials comprising the structure, with each of the corresponding order parameters penetrating into the other material. These effects follow from normal and Andreev³ reflection processes at the interfaces. In the latter process, an electron encounters one of the interfaces, is converted into a hole with opposite spin and traverses in the opposite direction. For S/N interfaces (where N is a nonmagnetic, nonsuperconducting metal) the dynamics of charge transport is degenerate with respect to the electron spin quantum variable. This is not true, however, in the case we consider here, where superconducting regions are separated by magnetic interlayers.

In SFS trilayers, as well as in multilayers built from a sequence of such structures (SFSFS...), the spin-splitting effect of the magnet produces important and nontrivial changes in Andreev and other scattering processes. The exchange field in the ferromagnet breaks the time-reversal symmetry and generates a superconducting state where the Cooper pairs acquire a finite momentum resulting in a spatial modulation of the superconducting pair amplitude in the F region.⁴ Depending on the geometric and material characteristics of the SFS trilayer, its thermodynamic equilibrium state can be a “0” or a “ π ” state, at zero current, depending on the value of the phase difference between the superconducting order parameters in the two S electrodes. It is this twofold possibility that lies at the foundation of the many spin-based switching phenomena, which in turn are the basis for devices, including superconducting π qubits⁵ and memory elements.⁶ For larger SFSFS,...,S type heterostructures the

order parameter may or may not flip between any pair of consecutive S layers, leading to a variety of possible configurations, which can be characterized as a sequence of 0 and π junctions.

Continual advances in nanoprocessing methods have made it possible to fabricate high quality structures containing SFS junctions, which have encouraged further study of these systems. From the thermodynamics point of view, a 0 to π transition as the temperature was varied was inferred⁷⁻⁹ from Josephson current measurements in Nb/CuNi/Nb junctions. The Josephson coupling in similar structures was also found to cross over from positive to negative, depending on the F layer thickness,¹⁰ indicating again a 0 to π switch. Under many experimental conditions, a change in the second-order Josephson coupling component was associated^{7,8,10} with the 0- π crossover while for other conditions⁹ the nonlinear current-phase relation did not reveal any change in the second-order Josephson coupling.

The thermodynamics of F/S structures has been directly examined largely in terms of studying the transition temperature to the normal state.¹¹⁻¹⁶ In the case of parallel magnetization alignment of the F layers, a first order phase transition to the normal state was demonstrated in short-period F/S superlattices,¹¹ and was later proposed¹² in spin-valve ferromagnet-superconductor-ferromagnet (FSF) nanostructures with thin F layers. For antiparallel orientation of the magnetization, the transition was shown to be always second order.¹³ The application of a bias voltage¹⁴ up to a critical value can cause the phase transition to be first order for both parallel and antiparallel alignments of the magnetization. For F/S bilayers with stripe domain structure,¹⁵ superconductivity appears via a first order transition. In some cases, with the action of an applied field, the compensating screening currents can enhance¹⁶ the superconducting state. The theoretical literature that examines the thermodynamic transitions between 0 and π configurations in SFS type structures is more sparse. It has been argued¹⁷ that the transition that takes place in Josephson junctions is discontinuous when the F layer thickness is uniform but it rounds off when it is vari-

able. To further understand the underlying competition between the various possible states and to better tailor these structures for practical applications, it is imperative to study the thermodynamics of systems potentially containing π junctions by investigating the parameters that may influence a first or second order phase transition from a 0 state to a π state or vice versa.

The objective of this paper is to clarify some of these issues by rigorously considering the thermodynamics of clean layered systems consisting of one or more SFS junctions so as to identify and characterize any phase transitions involving $0-\pi$ flipping. It has been shown at low-temperatures¹⁸ that for given S and F widths, exchange energy and other material parameters, multiple spatial configurations of the *self-consistent* pair amplitude can exist as local minima of the energy. The larger the number of layers, the more combinations were found to be possible. Among the various solutions, the ground state was found from accurate condensation energy computations. Here on the other hand, we have the more ambitious objective of studying the possible competing states as a function of temperature T through a careful analysis of the free energy differences. We find that, as T varies, phase transitions associated with flipping of SFS junctions from a 0 to a π state occur and that there is a discontinuity in the entropy at such transitions which, therefore, are of first order. We calculate the corresponding latent heat, and find that its magnitude is observable given current experimental capabilities.

We study layered F/S systems containing a number N_j of SFS junctions. We consider in particular $N_j=1$, the important case of a single junction, and, to show the richness and variety of the possible outcomes, also the case $N_j=3$. We compare as a function of T the condensation free energies of the competing self-consistent states. As explained in Sec. II below, this is not a trivial task. The numerical methods we use do resolve these small differences. In Sec. II, we explain how these calculations are carried out by using the spectra and pair potentials obtained by fully self-consistent numerical solution of the Bogoliubov-deGennes¹⁹ (BdG) equations and a convenient expression for the free energy. Results are presented in Sec. III, and comments and conclusions in Sec. IV.

II. METHODS

The systems studied here consist then of either 3 or 7 layers, containing 1 or 3 SFS junctions, respectively. We denote the thickness of the F layers by d_F and that of the S layers by d_S and assume the interfaces are sharp. We consider 3D slab-like heterostructures that are invariant in the $x-y$ plane and thus any spatial inhomogeneity occurs in the z direction. The BdG equations that determine the spin-up and spin-down quasiparticle amplitudes ($u_n^\uparrow, v_n^\downarrow$) and the associated eigenvalues, ϵ_n , take the form, in this quasi one dimensional case:

$$\begin{aligned} & \left[-\frac{1}{2m} \frac{\partial^2}{\partial z^2} + \epsilon_\perp - E_F(z) + U(z) - h(z) \right] u_n^\uparrow(z) + \Delta(z) v_n^\downarrow(z) \\ & = \epsilon_n u_n^\uparrow(z), \end{aligned} \quad (1a)$$

$$\begin{aligned} & - \left[-\frac{1}{2m} \frac{\partial^2}{\partial z^2} + \epsilon_\perp - E_F(z) + U(z) + h(z) \right] v_n^\downarrow(z) + \Delta(z) u_n^\uparrow(z) \\ & = \epsilon_n v_n^\downarrow(z), \end{aligned} \quad (1b)$$

where ϵ_\perp is the kinetic energy of the transverse modes, $\Delta(z)$ is the self-consistent pair potential, and $U(z)$ is the potential that accounts for scattering at each F/S interface. The ferromagnetic exchange energy $h(z)$ takes the constant value h in the F layers, and zero elsewhere. We assume parabolic bands: The variable bandwidth, $E_F(z)$, is characterized by the Fermi wavevector mismatch parameter defined as $\Lambda \equiv E_{FM}/E_{FS}$, where²⁰ E_{FS} is the Fermi energy in the S material, while in F we have $E_\pm \equiv E_{FM} \pm h$ for the majority (+) and minority (-) bands. A self-consistency condition¹⁸⁻²⁰ relates the spectrum obtained from Eq. (2) to the inhomogeneous pair potential $\Delta(z)$. The procedures that we use to numerically solve the BdG equations for a clean system in a fully self-consistent manner are detailed in Refs. 18 and 20 and the details need not be repeated here.

As explained in in Refs. 18 and 20, for many relevant values of the geometric and material parameters several self-consistent solutions, that is, local minima of the free energy, often coexist at $T=0$. For example, solutions¹⁸ of both the 0 and π type may be possible for one junction, while for the three junction case more than one of the possible symmetric states (000, $\pi\pi\pi$, $\pi 0\pi$, and $0\pi 0$ in the obvious notation denoting the state of each junction) may yield a self-consistent solution to the problem. In such cases, the equilibrium state had to be found by comparing the respective condensation energies. It was shown that the symmetry of the stable solution at $T=0$ can change¹⁸ as one varies parameters such as d_F , the interface barrier, the exchange field of the magnet, or the Fermi wavevector mismatch. The switchover from one stable state to another occurs as the corresponding energies cross at certain points in parameter space: ‘‘Phase transitions’’ take place as a function of such parameters. They may occur also in the dirty limit¹⁷ as a function of d_F . The issue is how these phenomena are related to transitions found experimentally⁷⁻¹⁰ at finite T .

When several competing self-consistent solutions occur, we must determine the equilibrium state by computing the condensation free energy $\Delta\mathcal{F}(T)$, defined as the difference $\Delta\mathcal{F}(T) \equiv \mathcal{F}_S(T) - \mathcal{F}_N(T)$ between the free energies of the normal and superconductor states of each of the several possible self-consistent configurations. It is in principle very difficult to compute condensation free energies to the required accuracy: One needs only to recall that in the bulk and at zero T , $\Delta\mathcal{F}$ equals²¹ $-(1/2)N(0)\Delta_0^2$ (Δ_0 is the bulk gap). Since \mathcal{F}_N is much larger, of order $N(0)\omega_D^2$ ($N(0)$ is the usual density of states at the Fermi surface for the S material, and ω_D the cutoff frequency), $\Delta\mathcal{F}$ is the small difference between two much larger quantities. Thus, one is faced with the tough numerical task of computing two quantities accurately enough so that the small difference between them can be reliably established. The problem is exacerbated for our systems because, as will be seen, the difference between the condensation free energies of the various possible states (e.g., the 0 and π cases for SFS trilayers) is at best a small

fraction of their individual condensation free energies. A particularly convenient expression for the free energy \mathcal{F} is given in Ref. 22:

$$\mathcal{F} = -2T \sum'_n \ln \left[2 \cosh \left(\frac{\epsilon_n}{2T} \right) \right] + \int_0^d dz \frac{|\Delta(z)|^2}{g}, \quad (2)$$

where d is the overall width of the system, g the usual superconducting coupling constant, and the prime on the sum indicates that only states of energy less than ω_D are included. This expression does not directly involve the eigenfunctions, which enter only indirectly through $\Delta(z)$ because of the self consistency condition.

Our investigation thus centers around the true thermodynamics, that is, how the equilibrium state of a given system depends on T , and the nature of the corresponding phase transitions. When self-consistent numerical solutions of the BdG equations are possible for multiple order parameter configurations, we evaluate the condensation free energies of the competing states. We find that in many cases there are first order phase transitions as a function of T , and that the latent heats are quite appreciable.

To locate phase transitions as a function of T , we searched near regions of parameter space where crossings occur¹⁸ at zero T . We focused on the Fermi wavevector mismatch parameter, d_F . For $N_j=1$ we take d_S equal to the zero temperature coherence length, ξ_0 , while for $N_j=3$ we double the thickness of the two inner S layers to $2\xi_0$. This mimics a more symmetric situation, since the outer layers are in contact with only one F layer. We measure energies in units of E_{FS} , lengths in units of k_{FS}^{-1} , the inverse of the Fermi wavevector for S, and set $k_{FS}\xi_0=100$. The strength of the magnet is chosen as $h=0.2E_{FM}$ throughout. We assume that all magnetic layers are aligned and that there is no oxide interlayer barrier ($U(z)=0$). We performed several checks of our numerical methods. For a system consisting of only one S layer with $d_S \gg \xi_0$, we quantitatively recover the textbook results²¹ for the thermodynamics, including the second order transition at the correct bulk value T_c^0 and associated specific heat discontinuity. This is a most stringent and severe test which confirms the capability of our numerical (and hence inherently finite-size) procedures to handle the fairly large systems (over four superconducting correlation lengths thick) that we study here. The low temperature limit was extensively checked in Ref. 18, and it was also previously verified²⁰ that our methods give the correct thickness dependence of $\Delta(z)$ for a superconducting slab as found in the literature.²³

III. RESULTS

Proceeding now to the results, consider first the case $N_j=1$. The top panel in Fig. 1 shows the condensation free energy $\Delta\mathcal{F}$, as defined above, normalized by $N(0)\Delta_0^2$, which is twice the value of the condensation energy for a bulk S material at $T=0$. The normalized free energy is plotted versus reduced temperature T/T_c^0 for both the 0 and π configurations of the one-junction system. These results correspond

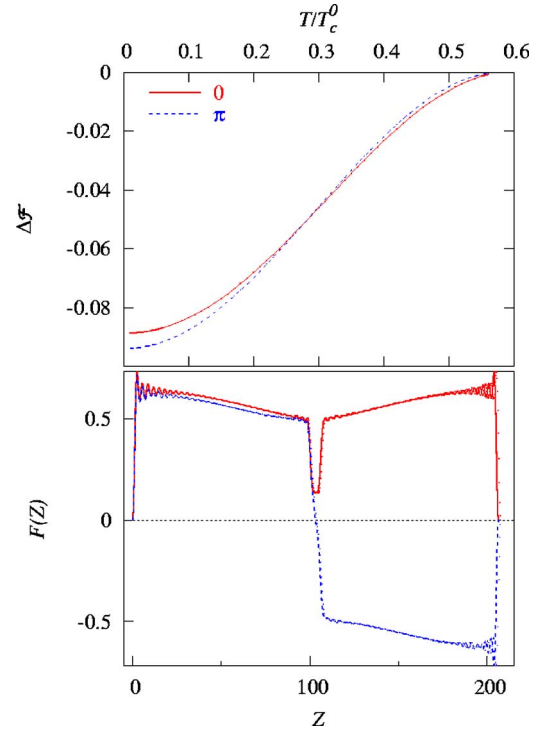


FIG. 1. (Color online) Normalized condensation free energy $\Delta\mathcal{F}$ (see text) as a function of reduced temperature, top panel, for a one junction (SFS) system at $\Lambda=0.535$ and $k_{FS}d_F=7.5$. Results for the two possible order parameter configurations are plotted as indicated. The lower panel displays the normalized pair amplitude $F(Z)$ (where $Z \equiv k_{FS}z$) at the transition point.

to $k_{FS}d_F=7.5$ and $\Lambda=0.535$. For these values, local minima of the free energy are found throughout the T range plotted for both the 0 and π configurations of $\Delta(z)$; similar results are found at this thickness for a range of Λ . Points at 0.01 intervals in the horizontal temperature scale are plotted, joined by straight segments. The slopes of the $\Delta\mathcal{F}$ curves approach zero as $T \rightarrow 0$, which indicates zero entropy at $T=0$. The slopes can also be seen to approach zero as $\Delta\mathcal{F} \rightarrow 0$: Thus we find that the transition to the normal state is second order, occurring at $T_c < T_c^0$. One can also see in the upper plot that the results for the 0 and π states cross at $T_x/T_c^0 \approx 0.28$, with the π configuration being the equilibrium state below T_x and the 0 state above. The difference in the slopes at T_x represents a latent heat, discussed below. Thus we predict that there is a transition and that it is first order. The lower panel displays the spatial profile of the corresponding pair amplitudes at T_x . The quantity plotted, $F(Z)$, is the pair amplitude as usually defined,¹⁹ normalized to its bulk S value at $T=0$. A large discontinuity in the absolute value of $F(Z)$ at the transition can be noted.

The next figure, Fig. 2, shows $\Delta\mathcal{F}(T)$ similarly plotted for a 3 junction (7 layer) system with $k_{FS}d_F=10$ and $\Lambda=0.45$. Points are again taken at intervals of 0.01 on the horizontal scale. In this case only two ($\pi\pi\pi$ and $\pi 0\pi$) of the possible configuration states compete¹⁸ as candidates for lowest free energy over the range of T studied. The other possible states are therefore irrelevant and omitted. The curves in the upper panel display the same characteristics as in the one-junction

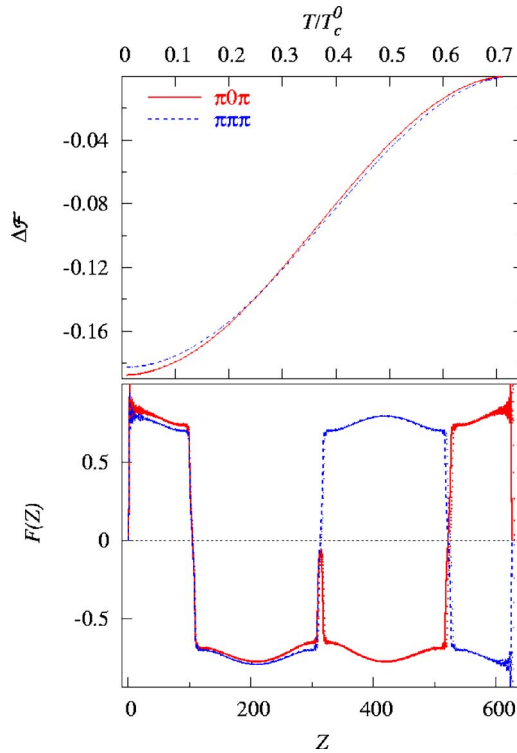


FIG. 2. (Color online) Results for a three junction system at $\Lambda = 0.45$ and $k_{FS}d_F = 10$. These plots are analogous to those in Fig. 1. The top panel shows results for the normalized condensation free energy. Only the two lowest competing free energy configurations are plotted. The lower panel displays the normalized pair amplitude $F(Z)$ for these two configurations at the transition point.

case: Zero first derivatives as $T \rightarrow 0$, a second order transition to the normal state, and a first order transition at an intermediate T . In this case the transition is at $T_x/T_c^0 \approx 0.27$ and from a $\pi 0 \pi$ state at lower T to $\pi \pi \pi$ at higher T . The lower panel again shows the corresponding $F(Z)$ at the transition. Thus in this more complicated example, the transition involves the inner 0 junction flipping to π as T is increased.

We can now derive the entire thermodynamics. Thus, Fig. 3 shows the dimensionless condensation entropies, $S(T)$, obtained by differentiating the results for $\Delta\mathcal{F}(T)$ (Figs. 1 and 2) with respect to T/T_c^0 . We show also the corresponding condensation energies, $U(T)$, computed from standard thermodynamic relations, normalized in the same way as $\Delta\mathcal{F}$. The top and bottom panels of Fig. 3 correspond, respectively, to the 1 and 3 junction cases in Figs. 1 and 2. As mentioned previously, the entropies go to zero smoothly as $T \rightarrow 0$ and $T \rightarrow T_c$. On the other hand, it is quite obvious that the transitions at T_x (vertical arrows) are indeed first order: The entropies of the two states involved are not equal at that temperature. The condensation energy curves resemble those for a bulk superconductor. By taking a further derivative, the specific heat can also be obtained. For any given state the quantities $S(T)$, $U(T)$, and $\Delta\mathcal{F}$ all go to zero at the same temperature, which is the computed value of T_c . The energies and entropies cross at temperatures above T_x : One can see that both entropy and energy play important and subtle roles in the first-order transition.

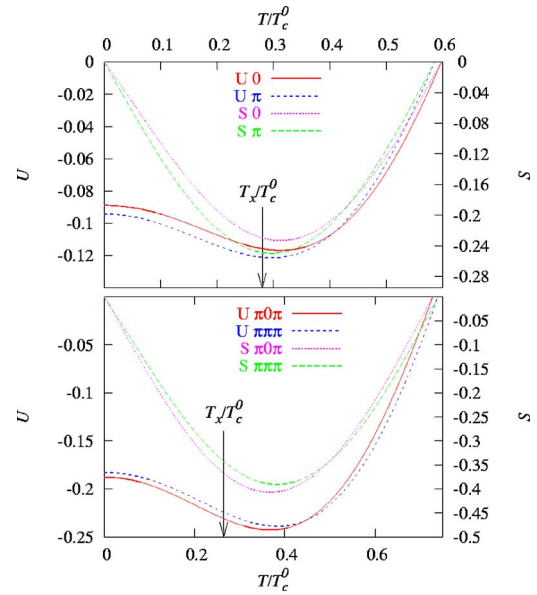


FIG. 3. (Color online) Dimensionless (see text) condensation entropy $S(T)$ (right scales) and energy $U(T)$ (left scales). Top and bottom panels correspond to the cases as in Figs. 1 and 2, respectively. The vertical arrows locate the first-order transitions.

These transitions occur, at fixed d_F , for a range of values of Λ : As one varies Λ , T_x moves up or down smoothly and monotonically until the transition disappears when T_x reaches either 0 or T_c . For the values of d_F and h used here, this range corresponds to $0.36 < \Lambda < 0.51$ for $N_J = 3$ and $0.52 < \Lambda < 0.55$ at $N_J = 1$. The difference between the entropies at $T = T_x$, which measures the latent heat, L , is quite appreciable and does not depend drastically on T_x (nor equivalently on Λ) over most of the range. These points are illustrated in Fig. 4, where L is shown for both the 1 and 3 junction systems. We show L (calculated as discussed in connection with Fig. 3) at several T_x . The sign of L is defined by subtracting the entropy of the stable state below T_x from that above T_x . So that the size of the effect can be appreciated, L is normalized to the specific heat at T_c^0 of a normal S material of the same volume. This is appropriate since for a normal metal the specific heat at T_c^0 equals its entropy. One can see

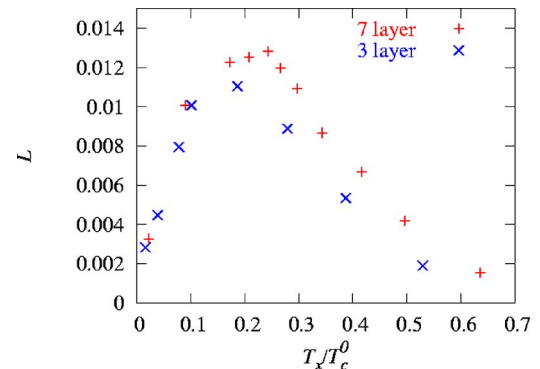


FIG. 4. (Color online) Variation of the latent heat with T_x . The entropy change, L , at T_x , normalized to the normal state specific heat at T_c^0 , is plotted as a function of T_x/T_c^0 for the one and three junction cases.

that, for both one and three junction samples, the entropy jumps at T_x can exceed 1% of the entropy present in a uniform bulk S sample at T_c^0 .

Translating these results for the normalized measure of the latent heat into actual units for typical samples,⁷ one can conservatively estimate they are of order of up to $10^{10}k_B T$ or 10^{-13} J. Standard ac calorimetry techniques offer a resolution^{24,25} at least one order of magnitude smaller. Therefore, these latent heats should be observable in single samples. Even attojoule calorimetry has been achieved in electronic systems, although by using multiple samples.²⁴ Our rigorous results are clearly larger than estimates made¹⁷ for dirty systems. These estimates, based on partial consideration of the Josephson energy only, are in the nature of lower bounds.

IV. SUMMARY AND CONCLUSIONS

In summary, we have rigorously studied the thermodynamics of clean single and triple SFS junction systems. Our results may be viewed as being complementary to those obtained in the more easily studied dirty limit¹⁷ to which they bear in some respects a qualitative similarity. We have shown

that as T is varied a given junction can flip from the 0 state to the π state. The resulting phase transition is first-order, in agreement with the experiments of Refs. 7, 8, and 10, for systems with sharp interfaces. In our calculations we have assumed that the thickness of the F layers is uniform. Variations in this quantity will produce some rounding off of the transition. One should remember, however, that a rounded-off first order transition is not the same as a second order, truly continuous one. Here (see bottom panels in Figs. 1 and 2) the pair potential, that is, the order parameter, undergoes a discontinuous change at T_x : The two states involved have different symmetry and there will be some degree of supercooling, superheating, or both. The associated latent heats were found to be within current experimental resolution. The results presented here should be applicable over a broad range of material parameters assuming d_S does not exceed several ξ_0 . Experiments in good clean samples to verify the existence of these transitions are most desirable.

ACKNOWLEDGMENTS

This work was supported in part by the University of Minnesota Graduate School and by the ARSC at the University of Alaska Fairbanks (part of the DoD HPCM program).

*Electronic address: barsic@physics.umn.edu

†Electronic address: otvalls@umn.edu

‡Electronic address: klaus.halterman@navy.mil

¹I. Žutić, J. Fabian, and S. Das Sarma, *Rev. Mod. Phys.* **76**, 323 (2004).

²A. I. Buzdin, B. P. Stojković, and O. T. Valls, *Rev. Mod. Phys.* **77**, 935 (2005).

³A. F. Andreev, *Sov. Phys. JETP* **19**, 1228 (1964) [*Zh. Eksp. Teor. Fiz.* **46**, 1823 (1964)].

⁴E. A. Demler, G. B. Arnold, and M. R. Beasley, *Phys. Rev. B* **55**, 15174 (1997).

⁵T. Yamashita, K. Tanikawa, S. Takahashi, and S. Maekawa, *Phys. Rev. Lett.* **95**, 097001 (2005).

⁶L. B. Ioffe, V. B. Geshkenbein, M. V. Feigel'man, A. L. Fauchere, and G. Blatter, *Nature (London)* **398**, 679 (1999).

⁷V. V. Ryazanov, V. A. Oboznov, A. Y. Rusanov, A. V. Veretennikov, A. A. Gulubov, and J. Aarts, *Phys. Rev. Lett.* **86**, 2427 (2001).

⁸H. Sellier, C. Baraduc, F. Lefloch, and R. Calemczuk, *Phys. Rev. Lett.* **92**, 257005 (2004).

⁹S. M. Frolov, D. J. Van Harlingen, V. A. Oboznov, V. V. Bolginov, and V. V. Ryazanov, *Phys. Rev. B* **70**, 144505 (2004).

¹⁰W. Guichard, M. Aprili, O. Bourgeois, T. Kontos, J. Lesueur, and P. Gandit, *Phys. Rev. Lett.* **90**, 167001 (2003).

¹¹Z. Radović, M. Ledvij, L. Dobrosavljević-Grujić, A. I. Buzdin, and J. R. Clem, *Phys. Rev. B* **44**, 759 (1991).

¹²I. Baladić and A. Buzdin, *Phys. Rev. B* **67**, 014523 (2003).

¹³S. Tollis, *Phys. Rev. B* **69**, 104532 (2004).

¹⁴B. Jin, G. Su, and Q. R. Zheng, *J. Appl. Phys.* **96**, 5654 (2004).

¹⁵V. L. Pokrovsky and H. Wei, *Phys. Rev. B* **69**, 104530 (2004).

¹⁶M. V. Milošević, G. R. Berdiyrov, and F. M. Peeters, *Phys. Rev. Lett.* **95**, 147004 (2005).

¹⁷A. Buzdin, *Phys. Rev. B* **72**, 100501(R) (2005).

¹⁸K. Halterman and O. T. Valls, *Phys. Rev. B* **69**, 014517 (2004).

¹⁹P. G. de Gennes, *Superconductivity of Metals and Alloys* (Addison-Wesley, Reading, MA, 1989).

²⁰K. Halterman and O. T. Valls, *Phys. Rev. B* **65**, 014509 (2002); **66**, 224516 (2002).

²¹M. Tinkham, *Introduction to Superconductivity*, 2nd ed. (Dover, New York, 2004).

²²I. Kosztin, Š. Kos, M. Stone, and A. J. Leggett, *Phys. Rev. B* **58**, 9365 (1998).

²³B. P. Stojković and O. T. Valls, *Phys. Rev. B* **49**, 3413 (1994); **50**, 3374 (1994), and references therein.

²⁴O. Bourgeois, S. E. Skipetrov, F. Ong, and J. Chaussy, B. P. Stojković, and O. T. Valls, *Phys. Rev. Lett.* **94**, 057007 (2005).

²⁵C. C. Huang, private communication.